A one-year comparison of new wind atlases over the North Sea

A one-year comparison of new wind atlases over the North Sea

Etienne Cheynet, Ida Marie Solbrekke, Jan Markus Diezel, Joachim Reuder
Geophysical Institute and Bergen Offshore Wind Centre, University of Bergen, Bergen, Norway
E-mail: etienne.cheynet@uib.no

Abstract. The New European Wind Atlas (NEWA) and the Norwegian hindcast archive (NORA3) database have become publicly available since the end of 2019 and mid-2021, respectively. They aim to model the long-term wind climatology with a spatial resolution of ca. 3 km and a temporal resolution of 1 h (NORA3) or 30 min (NEWA). Both products have a high potential for wind energy applications. Although their geographical coverages partly overlap, an inter-comparison of the NEWA and NORA3 databases in an offshore environment is still lacking. The paper compares the hourly mean wind speed and wind direction recorded in 2009 at the FINO1 platform (North Sea) with hindcast data from the NEWA and the NORA3 database. Both products were found to provide reliable estimates of the mean wind speed at 101 m above sea level. However, NORA3 shows slightly better performances than NEWA for the mean wind speed in terms of root-mean-square error, bias, earth mover's distance (EMD) and Pearson correlation coefficient. For the mean wind direction, a larger circular EMD than previously documented is found, which could be due to a directional bias in the wind vane data. Finally, the Brunt-Väisälä frequency is computed using sea-surface temperature analyses and the air temperature from NORA3 and NEWA at 101 m above sea level. The encouraging description of the static atmospheric stability by the wind atlases opens the possibility to study in more detail thermally-induced wind events for wind resource assessment or wind turbine design.

1. Introduction

Wind atlases generated from weather forecast models can be used to address two of the three "Grand Challenges in the science of wind energy", which were identified by Veers et al. [1]. The first challenge deals with the need to better understand the physics of the atmosphere at different scales. Wind atlases have been used in the past in combination with computational fluid dynamics to model the interaction between microscale and mesoscale atmospheric motion [2]. A realistic coupling between these spatial scales is crucial for wind resource assessment [3, 4], wind farm aerodynamics [5] and offshore wind turbine design [6]. The latter point belongs to the second Grand Challenge, which covers structural dynamics and the aerodynamics of wind turbines steadily increasing in size. Floating offshore wind turbines have vibrational frequencies close to or below 0.1 Hz [7], such that their dynamic and quasi-static response may be affected by both microscale and mesoscale wind velocity fluctuations, see e.g. Nybø et al [8].

State-of-the-art offshore wind turbines reach heights of more than 250 m, and thus considerably exceed the typical depth range of the surface layer of the marine atmospheric boundary layer (MABL) [9]. In that case, the logarithmic mean wind speed profile, traditionally used in, e.g., IEC61400-1 [10], or the power law wind profile is no longer an appropriate description of the mean flow conditions [11, 12]. By providing mean wind speed data in the first few hundred meters above the earth's surface, high-resolution

Table 1. Horizontal (Horiz. res.) and temporal resolution (Time res.) of the mean wind speed and direction from NORA3 and NEWA. Additional height levels are available from the complete NORA3 dataset, albeit with a temporal resolution of 3 h.

Source	Horiz. res. (km)	Time res. (min)	Height levels (m)
NORA3	3	60	10, 50, 100, 200, 300, 500, 750
NEWA	3	30	10, 50, 75, 100, 150, 200, 250, 500

wind atlases are valuable to overcome the limits of surface layer theory for wind turbine design and operation.

The New European Wind Atlas (NEWA) [13, 14] and the Norwegian Reanalysis NORA3 [15, 16] became available for open-access use in 2019 and 2021, respectively. Both NEWA and NORA3 can be considered state-of-the-art wind atlases as they permit the study of the wind climatology relevant to wind energy with an unprecedented high spatial and temporal resolution (table 1). However, to the author's knowledge, there exists no comparison between these wind atlases with in-situ atmospheric offshore measurements. Therefore, the present study aims to assess the reliability of both the NEWA and NORA3 datasets in the North Sea, using atmospheric data recorded on the FINO1 offshore platform in 2009. Several reasons justified the choice of the year 2009: (1) Since the beginning of 2010, the flow conditions around the FINO1 platform have been increasingly affected by wakes from wind turbines, deployed around the mast; (2) the earliest NEWA data were from 2009 at the time of this study was conducted (August 2021). The FINO1 platform was selected as a reference site as it has been extensively used to study the structure of the MABL for the last ten years [17, 18, 19]. Also, it is one of the few offshore masts in the North Sea that is instrumented with atmospheric sensors at multiple heights from 30 m above sea level (asl) to 101 m asl.

The present study is organized as follows: section 2 introduces the flow characteristics studied with the NORA3 and NEWA databases. A summary of the metrics used to compare both wind atlases is also provided. Section 3 compares the hourly mean wind speed and mean wind direction from NEWA and NORA3 with the data collected on the FINO1 platform by cup anemometers and wind vanes at heights between 51 m and 101 m above sea level (asl). It is shown that, for the year 2009, NORA3 slightly outperforms NEWA for the different metrics selected. Finally, the static atmospheric stability calculated using the two wind atlases and the sensors from the FINO1 platform is assessed in terms of probability density functions.

2. Data collection and analysis

2.1. The NEWA and NORA3 datasets

Both NORA3 and NEWA model the wind climatology in the first few hundred meters above the surface, with a spatial horizontal resolution of ca. 3 km and a time resolution equal to or finer than 1 h (table 1). These two wind atlases are based on the ERA5 reanalysis project [20] from the European Centre for Medium-Range Weather Forecasts (ECMWF). The latter is available at the Copernicus Climate Change Services [21] and provides climate and weather data globally with a horizontal spatial resolution of 31 km and a temporal resolution of 1 h. NEWA is based on the Weather Research and Forecasting (WRF) model whereas the regional numerical weather prediction model HARMONIE-AROME is used to create NORA3, as well as the Dutch Offshore Wind Atlas (DOWA) [22]. It should be noted, however, that DOWA covers a relatively small area compared to NORA3 or NEWA. Whereas NORA3 included data assimilation of the air temperature and relative humidity at 2 m above the surface [16] NEWA does not rely on data assimilation.

A subset of the NORA3 database with a hourly temporal resolution was selected and accessed through

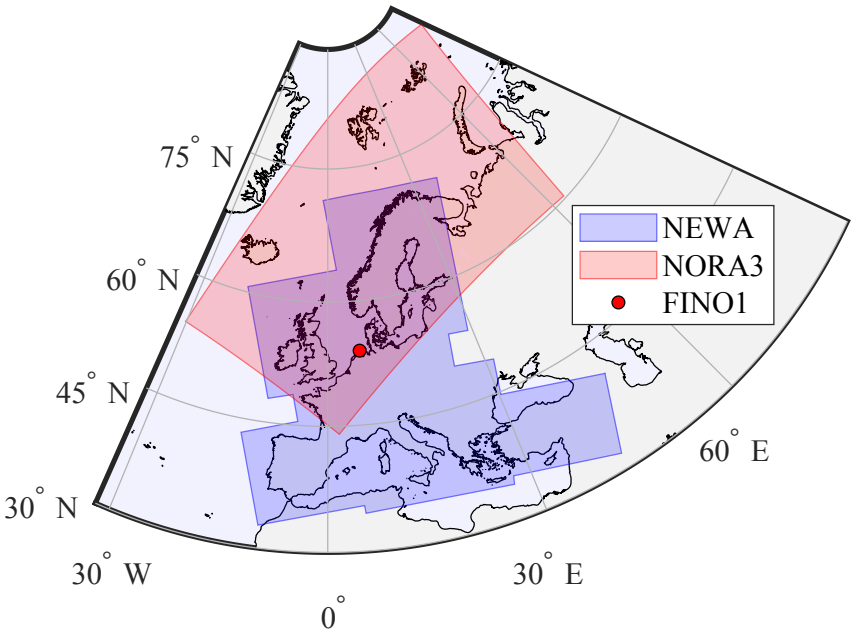

Figure 1. Simplified sketch of the domain covered by NEWA and NORA3 with the location of the FINO1 platform, located at $54.01°$ latitude and $6.57°$ longitude.

the OPeNDAP framework[1]. This subset provided profiles of the mean wind speed and mean wind direction at seven heights, from 10 m to 750 m asl. The complete NORA3 dataset provides additional vertical layers in a hybrid sigma-pressure coordinate scheme but with a 3-h temporal resolution. The NEWA data were also accessed using the OPeNDAP framework[2]. Both NORA3 and NEWA cover the North Sea and Baltic Sea (fig. 1), which make them ideally suited for offshore wind energy applications in Europe. Hereinafter, the NEWA and NORA3 datasets are simply referred to as NEWA and NORA3, respectively.

Although the atmospheric data provided by NORA3 and NEWA can be studied in the first 500 m above Earth's surface, their comparison is here limited to the first 100 m. This height corresponds to the highest position of the anemometers on the FINO1 platform. To ensure a consistent comparison between the data from FINO1 with the wind atlases, an averaging time of one hour is used for all three datasets. The original sampling time from the NEWA database and the sensors on the FINO1 platform is 30 min and 10 min, respectively. To obtain a sampling time of one hour, a moving average filter with a moving window of one-hour duration was first applied. Then, the data were linearly interpolated on an hourly time array.

2.2. The FINO1 platform

The FINO1 offshore platform ($54.014°$, $6.587°$) is located in the southern North Sea. It is instrumented with an extensive set of meteorological sensors, the list of which is available online [23]. For the sake of simplicity, table 2 summarizes those used in the present study only. The dataset was provided by the German Federal Maritime and Hydrographic Agency (BSH) as 10-min average records. The cup anemometers mentioned in table 2 were mounted on booms orientated with an angle from $135°$ to $142°$ from the North. Therefore, the anemometers were located in the mast shadow when the wind blew from west to northwest. The dataset used herein was corrected for the mast-induced flow distortion [24]. As shown in table 2, the mean wind speed data recorded by cup anemometers at two heights at 50 m and 101

[1] `https://thredds.met.no/thredds/projects/nora3.html`
[2] `http://opendap.neweuropeanwindatlas.eu/opendap/`

Table 2. Sensors from the FINO1 platform used for the comparison with the data from NORA3 and NEWA.

Sensor	Height asl (m)	Quantity	Support	Orientation (°)
Cup anemometer	51	Mean wind speed	Boom	140
Cup anemometer	101	Mean wind speed	Vertical strut	-
Sonic anemometer	62	Mean wind direction	Boom	308
Wind vane	91	Mean wind direction	Boom	315
Thermometer	101	Air temperature	Inside mast	-

m asl were selected for the mean wind speed data. For the wind direction, the measurements from the sonic anemometer at 62 m and the wind vane at 91 m were chosen.

2.3. Error assessment

Deviations between the two wind atlases and the in-situ data were studied using multiple metrics. For the mean wind speed, we used the Root-Mean-Square Error (RMSE), the bias and the first Wasserstein distance, also called earth Mover's distance (EMD) [25]. For the mean wind direction, the circular EMD (CEMD) was selected. Both the EMD and CEMD measure the distance between two probability distributions. They are included in the present study as they were two key metrics in the choice of the optimal setup for the NEWA dataset. For the sake of reproducibility, the numerical implementation of the CEMD is identical to the one used in Hahmann et al. [13], which is based on the python wrapper PyEMD [26]. In the present study, the EMD and CEMD are applied to probability density functions (PDFs) computed using kernel density estimates. The latter provides smooth PDFs with limited sensitivity on the bin width. For the wind direction, a circular kernel distribution [27] was used to avoid a bias near the boundaries of the interval scale.

2.4. Static atmospheric stability

One of the primary goals of NEWA was to describe the climatology of a site in terms of distribution of the mean wind speed and mean wind direction [13]. For wind energy applications, the distribution of atmospheric stability conditions is also relevant. The stratification of the atmosphere plays a central role, both in the shape of the inflow profile and wake propagation within wind turbines and even wind farms [28, 29, 30]. In this regard, the stratification of the atmosphere can significantly affect the wind power production [31] and wind loading on large offshore wind turbines [32, 33].

The profile of the atmospheric temperature was also extracted from the NORA3 and NEWA databases with the same spatial and temporal resolution as described in table 1. For the subset of NORA3, the temperature was given as a function of 16 pressure levels from $1000\,\mathrm{hPa}$ to $50\,\mathrm{hPa}$. To transform pressure levels into height levels, a formula based on the hydrostatic approximation [34] was used:

$$P(z) = P_0 \left(1 + \frac{\Gamma z}{T_0}\right)^{-\frac{g}{\Gamma R_s}} \tag{1}$$

where P_0 is the surface pressure given by NORA3 and T_0 is the surface temperature taken as equal to the sea surface temperature (SST); $R_s = 287.053\,\mathrm{J\,kg^{-1}\,K^{-1}}$ is the gas constant for dry air; $\Gamma = -6.5 \times 10^{-3}\,\mathrm{K\,m^{-1}}$ is the lapse rate assumed constant in the first $11\,\mathrm{km}$ above the surface following the International Standard Atmosphere guideline. Although eq. (1) is a fairly simple approximation, it is deemed appropriate in the present study, which focuses on the atmosphere in the first few hundreds of meters above the surface.

For comparison purposes, the absolute air temperature estimated using NORA3 was interpolated at 101 m asl by fitting a third-order polynomial function to the temperature profiles from the surface to a

maximal height $z_{max} = 1400\,\mathrm{m}$ asl. The choice of z_{max} is motivated by the need to include enough data points to avoid overfitting. At the same time, the height should be low enough to minimize the influence of temperature data at high altitudes on the shape of the polynomial function in the first few hundred meters above the surface. In the present case, the maximal correlation coefficient between the temperature data from NORA3 and those from the thermometer installed on the top of the mast was obtained for $z_{max} = 1400\,\mathrm{m}$ asl.

In the present study, the static atmospheric stability was studied using the Brunt-Väisälä frequency (N). The Bulk Richardson number was not considered as large uncertainties can arise from the combination of errors from both the mean wind speed and temperature. The Brunt-Väisälä frequency N was calculated using the potential temperature at the surface and 100 m (or 101 m). For two heights z_1 and z_2, N^2 is defined as

$$N^2 = \frac{2g}{\theta(z_2) + \theta(z_1)} \frac{\theta(z_2) - \theta(z_1)}{z_2 - z_1} \tag{2}$$

where $g = 9.81\,\mathrm{ms}^{-2}$ is the gravitational acceleration and $\theta(z)$ is the potential temperature at height z. As shown by eq. (2), $N > 0$ in statically stable air. Although this frequency is not defined for statically unstable environment, it is sometimes used as a measure of the static stability [35]. Therefore, for a statically unstable air, $N = \sqrt{-N^2}$ is used hereinafter. In the present case, the height z_1 (eq. (2)) is set to zero and $\theta(z_1)$ is, therefore, the surface potential temperature. The latter was obtained by combining the SST and the surface pressure P_0 from NORA3. The SST data were provided by BSH using in-situ measurements from a Waverider MKIII buoy (WAVEC Datawell), located a few hundred meters away from FINO1. Alternatively, the GLobal Multi-scale Ultra-high Resolution SST analysis [36], denoted MUR SST herein, can be used. For the dataset considered, the MUR SST and SST recorded by the buoy are in excellent agreement with a squared Pearson coefficient $R^2 = 0.995$.

The MUR SST data are paired herein with NORA3 and NEWA only. On the other hand, when the measurements from the FINO1 platform are used, the SST data are taken from the buoy. This choice was motivated by the fact that the MUR SST data are available since 2002 with a much higher data availability than the buoy data. Therefore, more than one decade of data may be used to study the static stability of the atmosphere in the North Sea by combining the NORA3 or NEWA database and the MUR SST analysis. However, such an application requires first to be validated against in-situ measurements, which are here taken from the FINO1 platform.

3. Results

The hourly mean wind speed and direction at 51 m asl and 101 m asl recorded in 2009 by the cup anemometers on the FINO1 platform are compared to the data provided by NORA3 and NEWA in fig. 2.

The squared Pearson correlation coefficients between the measured and modelled wind speed at 101 m asl are 0.8 and 0.9 for NEWA and NORA3, respectively. The median deviation for the NORA3 database is $-0.11\,\mathrm{m\,s}^{-1}$ with the first and third quartile of the deviation at $-0.84\,\mathrm{m\,s}^{-1}$ and $0.59\,\mathrm{m\,s}^{-1}$, respectively. For the NEWA dataset, the median, first quartile and third quartile deviation are $-0.31\,\mathrm{m\,s}^{-1}$, $-1.39\,\mathrm{m\,s}^{-1}$ and $0.80\,\mathrm{m\,s}^{-1}$, respectively. The bias found for the NORA3 database in 2009 is relatively close to the value of $-0.14\,\mathrm{m\,s}^{-1}$ estimated by Solbrekke et al. [15] using data between 2004 and 2016 and a different data processing.

Figure 3 shows the probability density function (PDF) of the mean wind speed recorded by the anemometer at 101 m asl in 2009 and the associated hindcast data from NORA3 and NEWA for the same period and same height. An additional panel covering 30 years of data, from 1985 to 2015, corresponds to the ERA5 reanalysis dataset at 101 m asl [21]. A quantile-quantile plot (not shown here) between the measured and modelled mean wind speed showed a nearly perfect linear relationship. It indicates that, for the period selected, the two wind atlases produce a similar mean wind speed distribution as the anemometers at 51 m and 101 m asl. The kernel distribution estimates are fitted by a Weibull distribution, the shape and scale parameters of which are denoted a and b, respectively. These parameters

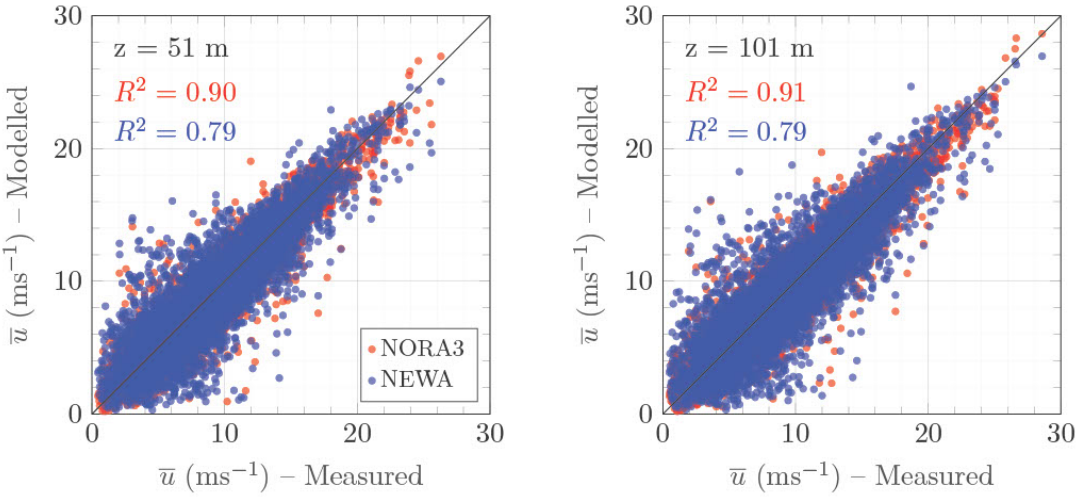

Figure 2. Hourly mean wind speed at 51 m (left panel) and 101 m (right panel) estimated by NORA3 and NEWA compared to cup anemometer measurements from the FINO1 platform. Each dot represents one hour of data, collected from 2009-01-01 to 2009-12-31.

are remarkably close between the FINO1 data and those estimated based on NORA3 and NEWA. The relative difference for a and b is only $-0.9\,\%$ and $0.4\,\%$, respectively, for NORA3 and $-2.8\,\%$ and $-0.8\,\%$, respectively, for NEWA. If the period between 1985 and 2015 is considered using the ERA5 database, the shape and scale parameters of the fitted Weibull distribution shows larger deviations than during the year 2009. It is unclear whether such differences are due to the limited accuracy of the ERA5 data or the fact that the climatology of the site is insufficiently represented by the year 2009 alone. A further study could use the entire period covered by NORA3 and NEWA (when openly available) from 1989 to 2019 to clarify this point.

The probability density functions of the mean wind direction are shown in a polar coordinate system in fig. 4 for the wind atlases and the FINO1 data for the year 2009. In the right panel, the ERA5 data at 101 m asl are also included for the sake of completeness. The directional bias was calculated as a circular distance [37]. A value of ca. $-9°$ was found between the hindcast data and the records from the wind vane at 91 m. The bias was only $-5°$ when the sonic anemometer data at 62 m were considered. Therefore, the calibration of the wind vane and sonic anemometer may differ by a few degrees. The CEMD value found in table 3 is larger than in Hamann et al. [13] and may reflect the presence of a bias in the wind vane data. More generally, the EMD and CEMD do not differentiate deviations due to a systematic bias between two distributions and deviations due to different distribution shapes. If possible, the EMD and CEMD could be further refined into unbiased and biased estimates when comparing numerical models and in-situ measurements. The study by Hamann et al. [13] did not include a detailed directional bias analysis and it is, therefore, unclear whether the CEMD values they found are unbiased or not. It can be noted that in fig. 4, the wind direction recorded at 62 m and 91 m are affected by mast-induced flow distortion when the wind blows from south-east. However, no significant deviations from the hindcast data are observed for the south-eastern sector, partly because the mean flow characteristics were corrected for the mast shadowing effect [24]. The Alpha Ventus wind park was commissioned in mid-November 2009. Therefore, it is unclear whether the discrepancies between the modelled and measured wind direction at 91 m are due to wind-turbine wakes or different instrument setups at 62 m and 91 m.

Deviations between the wind atlases and the cup anemometer on the FINO1 platform may be due to, e.g., significant mean wind speed variation within one hour or thermally driven wind speed profiles. The influence of the swell on the mean wind speed profile was not clearly visible at 50 m and 100 m asl, even for weak wind conditions ($\overline{u} \leq 5\,\mathrm{m\,s^{-1}}$) [38], which have limited interest for wind turbine operations

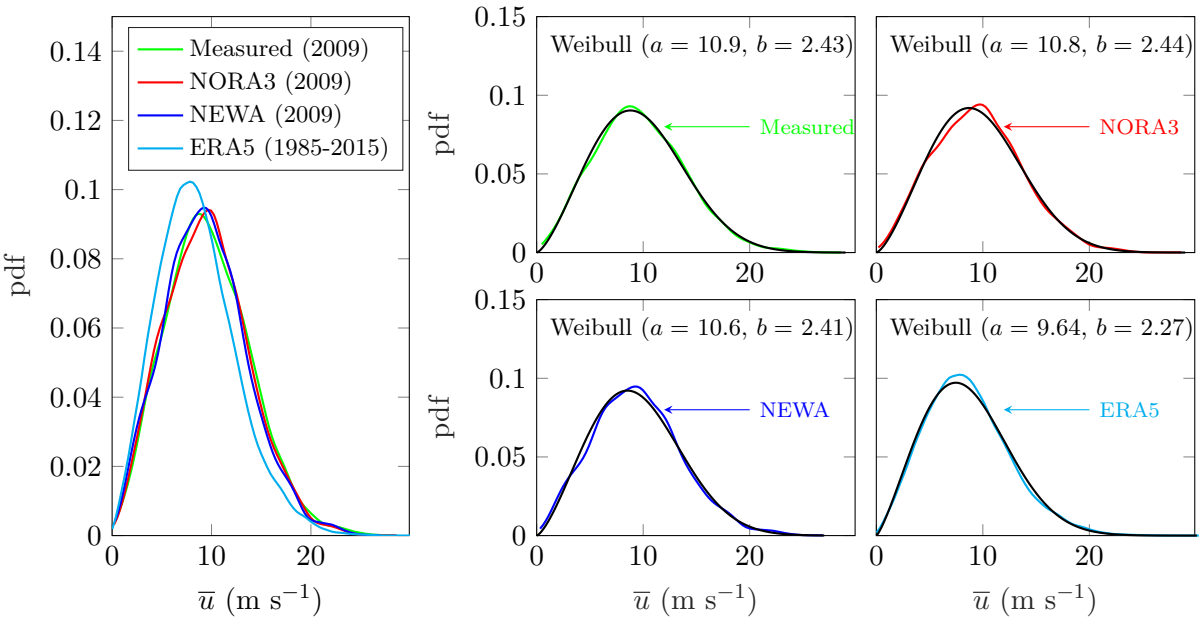

Figure 3. Distribution of the mean wind speed at 100 m asl in 2009, measured on the FINO1 platform (—), modelled by NORA3 (—), NEWA (—) and ERA5 (—) for the period 1985-2015. The solid black lines correspond to least-square fit of a Weibull distribution, the shape and scale parameters of which are denoted a and b, respectively.

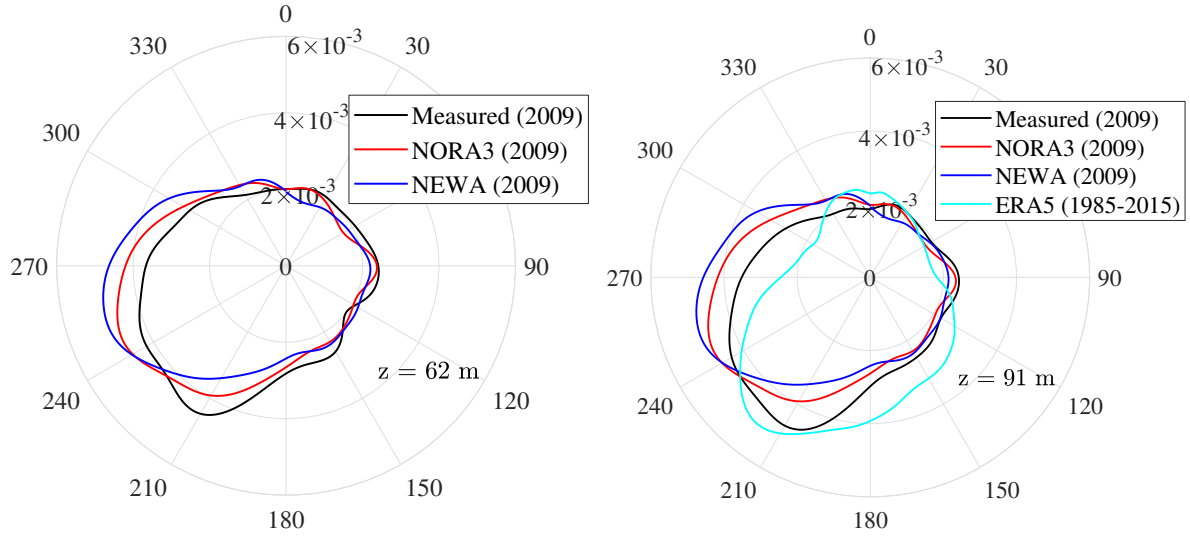

Figure 4. Probability density function (pdf) of the mean wind direction at 62 m asl (left) and 91 m asl (right) for the year 2009 at FINO1, computed using the in-situ measurements and the data from NEWA and NORA3. The pdf of the wind direction from the ERA5 data between 1985 and 2015 is also shown at 100 m asl for the sake of completeness.

since the cut-in wind speed is usually around 5 m s^{-1} at hub height.

To assess the temporal variability of the mean wind flow within one hour, the central difference of the 10-min wind speed time series, denoted $\partial\overline{u}$, was calculated using the cup anemometer data at 100

Table 3. Metrics used to assess the performances of NORA3 and NEWA compared to the measurements from the FINO1 platform in terms of mean wind speed at 101 m and wind direction at 91 m asl. Hourly data were collected from 2009-01-01 to 2009-12-31 (8739 samples). EMD stands for earth Mover's distance, CEMD is the circular EMD, RMSE is the root-mean square error and R is the Pearson correlation coefficient.

Models	Wind speed metrics				Wind direction metric
	EMD (m s^{-1})	RMSE (m s^{-1})	Bias (m s^{-1})	R^2	CEMD (°)
NORA3	0.13	1.3	-0.11	0.90	5.8
NEWA	0.26	2.0	-0.31	0.79	7.0

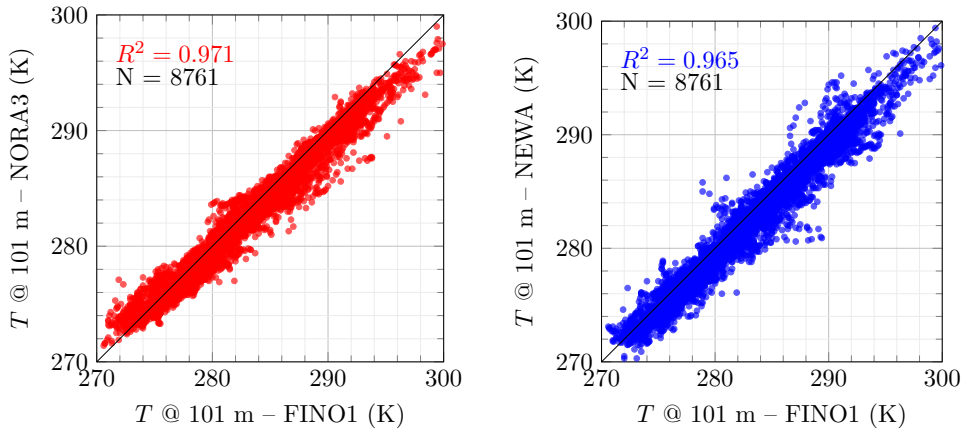

Figure 5. Absolute air temperature T at 101 m asl on the FINO1 platform compared to the values computed using NORA3 (left) and NEWA (right). Each dot represents one hour of data, collected from 2009-01-01 to 2009-12-31.

m asl. The Samples associated with a $|\partial\overline{u}|$ value above the 95$^{\text{th}}$ percentile ($0.4\,\text{m}\,\text{s}^{-1}$) were flagged as "non-stationary". For the NORA3 data, if the flagged data are removed, the squared Pearson correlation coefficient R^2 increases from 0.91 to 0.92 only. On the other hand, 63% (54%) of the data associated with a bias above $5\,\text{m}\,\text{s}^{-1}$ ($4\,\text{m}\,\text{s}^{-1}$) are flagged as non-stationary. Hindcast data with an absolute bias above $5\,\text{m}\,\text{s}^{-1}$($4\,\text{m}\,\text{s}^{-1}$) corresponds to only 0.5% (1.2%) of the selected subset of the NORA3 database. Although rare, such large deviations may, therefore, be partly explained by wind speed variations on a time scale much shorter than one hour.

3.1. Distribution of the static atmospheric stability

To assess the ability of NORA3 and NEWA to describe the distribution of the static stability near the FINO1 platform, a comparison with the air temperature collected at 100 m on the mast is first conducted. Figure 5 shows a R^2 of 0.97 for both NEWA and NORA3, with a bias of $-0.9\,\text{K}$ and $-0.6\,\text{K}$ for NEWA and NORA3, respectively. The average temperature bias is not expected to have a significant influence on the estimation of static stability. The lower uncertainties associated with the air temperature justify the use of the Brunt-Väisälä frequency N rather than e.g. the bulk Richardson number to study the stability of the atmosphere above the sea. Figure 6 shows the pdf of N computed with a kernel estimator. A similar comparison was done by Barstad [39] for the FINO1 platform with a 3 km gridded dataset downscaled from the ERA-Interim reanalysis using the WRF model and one year of data (2008). The Brunt-Väisälä frequencies estimated with NORA3 and NEWA have a better agreement with the FINO1 data than the

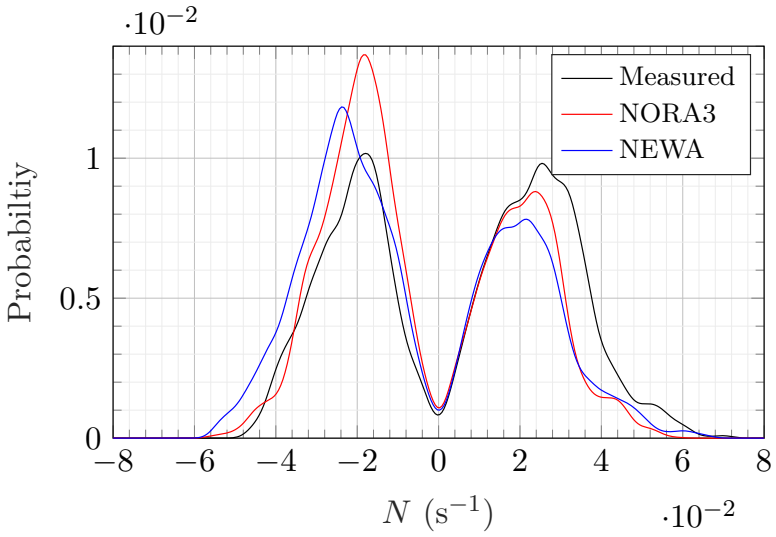

Figure 6. Probability density function of the Brunt-Väisälä frequency N computed using the potential temperature of the air at ca. 100 m asl and the sea surface temperature. Data from 2009-01-01 to 2009-12-31 near and/or on the FINO1 platform were used.

downscaling approach adopted by Barstad [39], especially under stable conditions. The EMD value for N was 0.006 for NORA3 and 0.008 for NEWA, suggesting that both models performed equally well.

4. Conclusions

The paper compared the performances of two state-of-the-art wind atlases, NORA3 and NEWA, in terms of mean wind speed, mean wind direction and static atmospheric stability. The reference data were taken from the offshore platform FINO1 in the southern North Sea. The mean wind speed provided at 101 m above the surface by both wind atlases compared well with the in-situ data, with a bias lower than $0.3\,\mathrm{m\,s^{-1}}$, a root-mean-square error under $2\,\mathrm{m\,s^{-1}}$, an earths mover distance under $0.3\,\mathrm{m\,s^{-1}}$ and a squared Pearson coefficients above 0.8. For these metrics, NORA3 slightly outperformed NEWA. A similar conclusion was obtained in terms of the circular earths mover distance for the mean wind direction.

The static atmospheric stability was estimated by combining atmospheric temperature from NORA3 (or NEWA) and high-resolution sea surface temperature from satellite observations. Both models performed equally well compared to the in-situ measurements, especially for near neutral and moderately diabatic conditions.

The preliminary findings of the present study provide a promising insight toward improved offshore wind assessment in the North Sea and the Norwegian sea. Additional validation studies of NORA3 against in-situ data offshore and onshore at an altitude higher than 100 m above ground are currently conducted. They will provide a more complete picture of the potential of this wind atlas in northern Europe, especially on the Norwegian coast, for airborne and offshore wind energy applications as well as meteorological applications.

Acknowledgements

The Federal Maritime and Hydrographic Agency of Germany (BSH) is acknowledged for providing the FINO1 data, available at `http://fino.bsh.de/`. We are grateful to Dr Andrea Hahmann and Dr Bjarke Tobias Olsen for their help regarding the implementation of the circular EMD function. Parts of this work have been supported by funding from the European Union Horizon 2020 through the Innovation Training Network Marie Skłodowska-Curie Actions: Lidar Knowledge Europe (LIKE (grant no. 858358))

References

[1] Veers P, Dykes K, Lantz E, Barth S, Bottasso C L, Carlson O, Clifton A, Green J, Green P, Holttinen H, Laird D, Lehtomäki V, Lundquist J K, Manwell J, Marquis M, Meneveau C, Moriarty P, Munduate X, Muskulus M, Naughton J, Pao L, Paquette J, Peinke J, Robertson A, Sanz Rodrigo J, Sempreviva A M, Smith J C, Tuohy A and Wiser R 2019 *Science* **366** eaau2027
[2] Mughal M O, Lynch M, Yu F and Sutton J 2018 *J. Wind Eng. Ind. Aerodyn.* **176** 13–20
[3] Beaucage P, Brower M C and Tensen J 2014 *Wind Energy* **17** 197–208
[4] Haupt S E, Kosovic B, Shaw W, Berg L K, Churchfield M, Cline J, Draxl C, Ennis B, Koo E, Kotamarthi R *et al.* 2019 *Bull Am Meteorol Soc* **100** 2533–2550
[5] Gopalan H, Gundling C, Brown K, Roget B, Sitaraman J, Mirocha J D and Miller W O 2014 *J. Wind Eng. Ind. Aerodyn.* **132** 13–26
[6] Sanz Rodrigo J, Chávez Arroyo R A, Moriarty P, Churchfield M, Kosović B, Réthoré P E, Hansen K S, Hahmann A, Mirocha J D and Rife D 2017 *Wiley Interdiscip. Rev. Energy Environ* **6** e214
[7] Nielsen F G, Hanson T D and Skaare B 2006 Integrated dynamic analysis of floating offshore wind turbines *International conference on offshore mechanics and arctic engineering* vol 47462 pp 671–679
[8] Nybø A, Nielsen F G and Godvik M 2021 *Wind Energy*
[9] Liu S and Liang X Z 2010 *J. Clim.* **23** 5790–5809
[10] IEC 61400-1 2005 IEC 61400-1: Wind Turbines–Part 1: Design Requirements
[11] Lange B, Larsen S, Højstrup J and Barthelmie R 2004 *J. Wind Eng. Ind. Aerodyn.* **92** 959–988
[12] Peña A, Gryning S E and Hasager C B 2008 *Boundary Layer Meteorol* **129** 479–495
[13] Hahmann A N, Sīle T, Witha B, Davis N N, Dörenkämper M, Ezber Y, García-Bustamante E, González-Rouco J F, Navarro J, Olsen B T *et al.* 2020 *Geosci. Model Dev.* **13** 5053–5078
[14] Dörenkämper M, Olsen B T, Witha B, Hahmann A N, Davis N N, Barcons J, Ezber Y, García-Bustamante E, González-Rouco J F, Navarro J *et al.* 2020 *Geosci. Model Dev.* **13** 5079–5102
[15] Solbrekke I M, Sorteberg A and Haakenstad H 2021 *Wind Energy Sci.* **6** 1501–1519
[16] Haakenstad H, Breivik Ø, Furevik B R, Reistad M, Bohlinger P and Aarnes O J 2021 *J Appl Meteorol Climatol*
[17] Türk M and Emeis S 2010 *J. Wind Eng. Ind. Aerodyn.* **98** 466–471
[18] Kettle A J 2014 *J. Wind Eng. Ind. Aerodyn.* **134** 149–162
[19] Cheynet E, Jakobsen J B and Reuder J 2018 *Boundary Layer Meteorol* **169** 429–460
[20] Hersbach H, Bell B, Berrisford P, Hirahara S, Horányi A, Muñoz-Sabater J, Nicolas J, Peubey C, Radu R, Schepers D *et al.* 2020 *Q J R Meteorol Soc* **146** 1999–2049
[21] Hersbach H, Bell B, Berrisford P, Biavati G, Horányi A, Muñoz Sabater J, Nicolas J, Peubey C, Radu R, Rozum I *et al.* 2020 ERA5 hourly data on single levels from 1979 to present accessed on 10-01-2020. doi:10.24381/cds.adbb2d47
[22] Kalverla P C, Holtslag A A, Ronda R J and Steeneveld G J 2020 *Q J R Meteorol Soc* **146** 1498–1515
[23] UL International GmbH – DEWI 2015 Fino1 – meta data. `https://www.bsh.de/DE/THEMEN/Beobachtungssysteme/Messnetz-MARNET/FINO/_Anlagen/Downloads/FINO1_metadata.pdf?__blob=publicationFile&v=3` last accessed: 29-09-2021
[24] Westerhellweg A, Neumann T and Riedel V 2012 *DEWI-Magazin* **21**
[25] Rubner Y, Tomasi C and Guibas L J 2000 *Int. J. Comput. Vis.* **40** 99–121
[26] Pele O and Werman M 2008 A linear time histogram metric for improved sift matching *Computer Vision–ECCV 2008* (Springer) pp 495–508
[27] Atanasiu V 2021 Kernel smoothing density estimate for circular data (`https://se.mathworks.com/matlabcentral/fileexchange/32614`) MATLAB Central File Exchange. Retrieved September 29, 2021
[28] Hansen K S, Barthelmie R J, Jensen L E and Sommer A 2012 *Wind Energy* **15** 183–196
[29] Dörenkämper M, Witha B, Steinfeld G, Heinemann D and Kühn M 2015 *J. Wind Eng. Ind. Aerodyn.* **144** 146–153
[30] Platis A, Siedersleben S K, Bange J, Lampert A, Bärfuss K, Hankers R, Cañadillas B, Foreman R, Schulz-Stellenfleth J, Djath B *et al.* 2018 *Sci. Rep.* **8** 1–10
[31] Guo N, Zhang M, Li B and Cheng Y 2021 *J. Wind Eng. Ind. Aerodyn.* **211** 104548
[32] Sathe A, Mann J, Barlas T, Bierbooms W and Van Bussel G 2013 *Wind Energy* **16** 1013–1032
[33] Jacobsen A and Godvik M 2021 *Wind Energy* **24** 149–161
[34] ISO 2533:1975 1975 Standard Atmosphere Tech. rep. International Organization for Standardization Geneva, Switzerland
[35] Stull R B and Ahrens C D 1995 *Meteorology today for scientists and engineers* (West Pub.)
[36] JPL MUR MEaSUREs Project 2015 Ghrsst level 4 mur global foundation sea surface temperature analysis (v4.1). ver. 4.1. po.daac, ca, usa dataset accessed [2020-01-28] at https://doi.org/10.5067/GHGMR-4FJ04
[37] Berens P 2021 Circular statistics toolbox (directional statistics) (`https://se.mathworks.com/matlabcentral/fileexchange/10676`) MATLAB Central File Exchange. Retrieved September 29, 2021
[38] Sjöblom A and Smedman A S 2003 *Boundary Layer Meteorol* **109** 1–25
[39] Barstad I 2016 *Wind Energy* **19** 515–526